Vanadium isotope measurement by MC-ICP-MS

Fei Wu, Yuhan Qi, Huimin Yu, Shengyu Tian, Zhenhui Hou, Fang Huang *

CAS Key Laboratory of Crust-Mantle Materials and Environments, School of Earth and Space Sciences, University of Science and Technology of China, Hefei 230026, Anhui, China

ABSTRACT

We present a method to measure vanadium (V) isotopic composition for terrestrial rocks in this study. Vanadium was efficiently separated from matrix elements by a chromatographic technique using cation- and anion-exchange resin columns, avoiding the expensive TRU Spec resin. Vanadium isotope ratios were measured using a Thermo Scientific Neptune Plus MC-ICP-MS employing a sample–standard bracketing method. The increase in instrument sensitivity significantly reduces the amount of V required for the isotope analysis. Potential effects of acid molarities and concentration mismatch on instrumental analyses were rigorously evaluated. In addition, we performed Cr- and Ti-doping experiments to ensure the precision and accuracy of V isotope measurement. The $\delta^{51}V$ values of mono-elemental V standards (BDH and USTC-V) relative to an Alfa Aesar (AA) standard solution (defined as $\delta^{51}V = [(^{51}V/^{50}V)_{sample} / (^{51}V/^{50}V)_{AA} - 1] \times 1000$) measured in our laboratory were $-1.23 \pm 0.08\text{‰}$ (2 SD, $n = 197$) and $0.07 \pm 0.07\text{‰}$ (2 SD, $n = 112$), respectively. Analyses of synthetic standard solutions (element doping + matrix spiking) obtained the same $\delta^{51}V$ for the pure V solutions with a precision better than $\pm 0.1\text{‰}$ (2 SD). Vanadium isotopic compositions of 12 reference materials, including igneous rocks (with mafic to felsic compositions) and manganese nodules, were measured using this method. These reference materials including basalts: BCR-2, $-0.78 \pm 0.08\text{‰}$ (2 SD, $n = 36$); BHVO-2, $-0.83 \pm 0.09\text{‰}$ (2 SD, $n = 22$); BIR-1, $-0.92 \pm 0.09\text{‰}$ (2 SD, $n = 52$); JB-2, $-0.87 \pm 0.06\text{‰}$ (2 SD, $n = 20$); diabase: W-2, $-0.94 \pm 0.08\text{‰}$ (2 SD, $n = 15$); andesites: AGV-1, $-0.71 \pm 0.10\text{‰}$ (2 SD, $n = 6$); AGV-2, $-0.70 \pm 0.10\text{‰}$ (2 SD, $n = 37$); JA-2, $-0.80 \pm 0.07\text{‰}$ (2 SD, $n = 15$); quartz latite: QLO-1, $-0.61 \pm 0.03\text{‰}$ (2 SD, $n = 3$); granodiorite: GSP-2, $-0.62 \pm 0.07\text{‰}$ (2 SD, $n = 26$); and manganese nodules: NOD-P, $-1.65 \pm 0.06\text{‰}$ (2 SD, $n = 10$); NOD-A, $-0.99 \pm 0.10\text{‰}$ (2 SD, $n = 19$). Based on repeated analyses of the rock standards, the long-term external precision of our method is better than $\pm 0.1\text{‰}$ (2 SD) for $\delta^{51}V$. Such precision allows us to identify V isotope fractionation in high-temperature terrestrial samples, suggesting that V isotope geochemistry can be more widely used to study magmatism as well as supergene processes.

© 2015 Published by Elsevier B.V.

1. Introduction

Vanadium (V) is a transition metal with multiple valence states (V^{5+}, V^{4+}, V^{3+}, and V^{2+}) in nature. The proportion of vanadium with different valence states in the planetary basaltic melts and mantle peridotites is related to oxygen fugacity of the systems (e.g., Papike et al., 2005). The chemical speciation and solubility of V in water are strong functions of pH and Eh conditions (e.g., Baes and Mesmer, 1976; Takeno, 2005; Zhou et al., 2011). Therefore, vanadium has been widely used to constrain variations of redox conditions during many geological processes (Huang et al., 2015 and references therein). For example, vanadium concentrations of the bulk earth versus bulk silicate earth (BSE) have been used to understand the conditions of terrestrial accretion and core formation (e.g., Siebert et al., 2013; Wood et al., 2008). Furthermore, vanadium concentrations and its ratios relative to single valent elements with similar compatibility in peridotites and

mantle-derived magma have been used as a proxy for redox condition variations of the mantle (e.g., Canil, 2002; Lee et al., 2005; Mallmann and O'Neill, 2009). Vanadium is significantly enriched in carbonaceous rocks or materials (up to 10,000 ppm) (Breit and Wanty, 1991), which can be used to trace marine oxidation state (e.g. Algeo and Maynard, 2004; Morford and Emerson, 1999). In addition, vanadium can be significantly enriched into crude oil, and the value of V / (V + Ni) is commonly used to determine crude oil grade (e.g., Ventura et al., 2015, and references therein).

Vanadium has two stable isotopes (^{51}V and ^{50}V) with relative abundances of ~99.76% and ~0.24%, respectively (Shore et al., 2010). Theoretical investigation and experimental studies have shown that isotopes of multi-valence elements can be fractionated during redox reactions (e.g., Anbar et al., 2005; Ellis et al., 2002; Schauble et al., 2004). Recently, first-principle calculations predicted that large V isotope fractionation could occur during V transportation and segregation in natural solutions via redox reaction and adsorption processes (Wu et al., 2015). Thus, V isotopic compositions of terrestrial samples may also fingerprint redox-state variations in nature.

Vanadium isotopes were analyzed using thermal ionization mass spectrometry (TIMS) in early studies (Balsiger et al., 1969; Balsiger et al., 1976; Pelly et al., 1970). Because of large uncertainty of V isotopes measurement (>1‰), no isotope difference between terrestrial matters and meteoritic samples could be observed at that time. However, chromatographic experiments have implied that V isotope fractionation would occur at low temperature (Zhang et al., 2003a, 2003b).

Analytical development based on application of MC-ICP-MS over the last two decades has dramatically expanded the feasibility of high-precision stable isotope analyses in the periodic table. However, application of V isotope geochemistry is still in its infancy. The main obstacles to precise and accurate V isotope measurements by MC-ICP-MS include: (1) the double-spike method cannot be applied to correct the instrument fractionation of V isotopes because V only has two stable isotopes; (2) the high $^{51}V/^{50}V$ (~400) makes it difficult simultaneously to obtain stable signals for both ^{51}V and ^{50}V in MC-ICP-MS; (3) isobaric interferences from ^{50}Ti and ^{50}Cr on the minor ^{50}V isotope mean that the chemistry has to separate those elements effectively; and (4) multi-atom molecular interferences (e.g., $^{36}Ar^{14}N^+$, $^{36}Ar^{16}O^+$, $^{38}Ar^{14}N^+$) could produce erroneous isotope data.

Recently, highly precise and accurate V isotope data have been obtained with analysis precision better than ±0.15‰ (2 SD) (Nielsen et al., 2011; Prytulak et al., 2011). Vanadium isotopic data were reported in standard δ-notation in per mil relative to the AA V standard solution (Nielsen et al., 2011): $\delta^{51}V = 1000 \times [(^{51}V/^{50}V_{sample} / ^{51}V/^{50}V_{AA}) - 1]$. Studies on mantle xenoliths and mafic lavas gave an estimation of the V isotopic composition of the BSE, showing that V isotopes can be fractionated during high-temperature mantle-melting processes (Prytulak et al., 2013). Vanadium isotope measurements of meteorites indicate that the silicate Earth is enriched in ^{51}V by about 0.8‰ relative to chondrites, likely reflecting the different irradiation history of the Solar System (Nielsen et al., 2014). More recently, up to ~1.5‰ variation of $\delta^{51}V$ was observed in crude oils, implying the potential application of V isotope to constraining the biogeochemical cycling of V and understanding the formation and preservation of petroleum source rocks (Ventura et al., 2015).

Despite the development of V isotope measurement with MC-ICP-MS, a more efficient procedure for chemical separation of V is needed to explore V isotope variations in nature. Application of V isotope geochemistry to high-temperature processes requires to further improvement in the analytical precision. Furthermore, there is still a lack of adequate V isotope data of reference materials for inter-lab comparison.

In this study, we present a method to measure V isotopes using MC-ICP-MS by the sample-standard bracketing technique. A chemical procedure of V purification modified after Nielsen et al. (2011) improves the time efficiency and eliminates the use of expensive TRU Spec resin. The increase in instrument sensitivity greatly reduces the abundance requirement of V for isotope analysis. We measured V isotopic compositions of 12 reference materials rock standards including 10 igneous rock standards from the United States Geological Survey (USGS) and the Geological Survey of Japan (GSJ) and two manganese nodule standards from the USGS. The reference values for these geological reference materials are helpful for future inter-lab calibration and data quality control. Based on replicated analyses of solution standards and rock standards, our long-term external reproducibility for $\delta^{51}V$ is better than ±0.1‰ (2 SD).

2. Analytical methods

2.1. Sample dissolution

Chemistry purification was carried out in a class 1000 clean laboratory equipped with class 100 laminar flow exhaust hood. All concentrated high-purity acids (HCl, HNO₃ and HF) were made through double sub-boiling distillation of the trace grade acids from Thermo Fisher Scientific. Hydrogen peroxide (30% v/v, ultrapure, AUECC) and ultrapure water (18.2 MΩ·cm) were used during the experiment. Vanadium concentrations in the analyzed reference materials vary from ~50 to ~800 ppm. 20–100 mg samples were weighed to contain 5–10 μg V for isotopic analysis. The igneous rock standards were digested in a 3:1 (v/v) mixture of concentrated HF and HNO₃ in Savillex screw-top beakers by heating at 140 °C on a hotplate for about 3–4 days. After evaporation to dryness, samples were treated with aqua regia, 6 mol L⁻¹ HCl, and 8 mol L⁻¹ HNO₃ in sequence and dried to remove any remaining fluorides. For manganese nodules/crusts, samples were first treated with aqua regia in Savillex screw-top beakers by heating at 120 °C on a hotplate for about two days. After evaporation to dryness, samples were dissolved with a 3:1 (v/v) mixture of concentrated HF and HNO₃ to digest the remaining oxide and silicate phases. Then, aqua regia and 8 mol L⁻¹ HNO₃ were used to ensure that samples were totally dissolved. The final material was dissolved in 1 mL of 1 mol L⁻¹ HNO₃ for ion-exchange separation.

2.2. Ion-exchange chromatography

In this study, chemical separation of V was achieved in a multi-step ion-exchange procedure by coupling cation- and anion-exchange columns (Table 1).

2.2.1. Cation resin procedure

Vanadium purification was first performed in a pre-cleaned Bio-Rad Poly-Prep chromatography column (9 cm high and 2 mL bed volume) loaded with 2 mL of Bio-Rad AG50W-X12 (200–400 mesh) cation resin. Fig. 1 shows the elution curves for our V purification procedures. The cation-exchange resin column was used to remove Fe, Ti, and some major matrix elements (e.g., Al, Ca, Mn, and Cr). Before loading the resin into the columns, it was cleaned by rinsing and shaking with 6 mol L⁻¹ HCl and H₂O alternately for more than twice, and then 1 mol L⁻¹ HNO₃ and H₂O alternately at least twice. In addition, the loaded cation resin was cleaned with 20 mL 6 mol L⁻¹ HCl and 10 mL H₂O in sequence, and then conditioned with 3 mL 1 mol L⁻¹ HNO₃ twice prior to any use. The sample solution with 5–10 μg V in 1 mL 1 mol L⁻¹ HNO₃ was then loaded on the conditioned cation-exchange column. 4 mL of 1 mol L⁻¹ HNO₃ + 0.1 mol L⁻¹ HF and 1 mL 1.2 N HNO₃ were used to elute Ti and Al. Vanadium was then collected with 19 mL 1.2 mol L⁻¹ HNO₃. After this step, most matrix elements (e.g., Fe, Ca, most Mn, and Cr) were still retained on the column while V was quantitatively eluted. In general, such a cation-exchange procedure was run twice to ensure that Fe and Ti were totally removed.

Elution curves can shift with variations in the amount of target element loaded to the column (e.g., An et al., 2014). To achieve a 100% recovery rate of V for different type of samples, it is necessary to test if V elution curves drift with various loading sizes. As shown in Fig. 2, although elution curves of V shift with different amounts of V, 100% recovery rate of V could be achieved if no more than 10 μg V was loaded to the column. Besides, for each sample the aliquots before and after the "V-cut" were collected to monitor V leakage during the chromatography process. After such a cation-exchange procedure, the sample was evaporated to dryness and dissolved in 1 mL dilute HCl (<0.01 mol L⁻¹; pH 2–3). Because K, Na and Mg are the main matrix elements remaining after the cation-exchange procedures, it is easy to dissolve the sample completely in dilute HCl (<0.01 mol L⁻¹; pH 2–3), avoiding the somewhat time-consuming operation described by Prytulak et al. (2011). This step is important for the next anion-exchange step, which separates V from most other matrix elements.

2.2.2. Anion resin procedure

Further purification of V was achieved through anion-exchange columns. The procedure was modified after Nielsen et al. (2011) to remove residual matrix compounds (such as K, Na, Mg, and trace Cr). A pre-cleaned Bio-Rad Poly-Prep chromatography column (9 cm high and 2 mL bed volume) was filled with 1.4 mL of Bio-Rad AG1-X8

Table 1

V purification scheme.

Resin	Eluent	Vol. (ml)	Comment
2 mL AG50W-X12 (200–400 mesh)[a]	1 mol L^{-1} HNO$_3$	3 (×2)	Conditioning
	Load sample in 1 mol L^{-1} HNO$_3$	1	
	1 mol L^{-1} HNO$_3$ + 0.1 mol L^{-1} HNO3	4	Elute Ti, Al
	1.2 mol L^{-1} HNO$_3$	1[b]	Pre-cut collection
	1.2 mol L^{-1} HNO$_3$	19	Collect V
	1.2 mol L^{-1} HNO$_3$	1[b]	After-cut collection
1.4 mL AG1-X8 (200–400 mesh)	0.01 mol L^{-1} HCl + 1% v/v H$_2$O$_2$	3 (×2)	Conditioning
	Load sample in 0.01 mol L^{-1} HCl + 1% v/v H$_2$O$_2$	1	
	0.01 mol L^{-1} HCl + 1% v/v H$_2$O$_2$	15	Elute matrix elements
	1 mol L^{-1} HCl	17	Collect V
	6 mol L^{-1} HCl	3	Collect V
0.1 mL AG1-X8 (200–400 mesh)	0.01 mol L^{-1} HCl + 1% v/v H$_2$O$_2$	0.5 (×2)	Conditioning
	Load sample in 0.01 mol L^{-1} HCl + 1% v/v H$_2$O$_2$	1	
	0.01 mol L^{-1} HCl + 1% v/v H$_2$O$_2$	2	Elute matrix elements
	1 mol L^{-1} HCl	1.7	Collect V
	6 mol L^{-1} HCl	0.3	Collect V

[a] Cation-exchange procedure was run twice.
[b] Eluent was used to test whether there is a loss of V or not.

(200–400 mesh) chloride-form anion resin. Before loading it into the columns, the resin was cleaned by rinsing and shaking with 1 mol L^{-1} HNO$_3$ and H$_2$O alternately at least four times. The resin was loaded in the column and cleaned with 10 mL of 6 mol L^{-1} HCl, 10 mL of 1 mol L^{-1} HNO$_3$, 10 mL of ultrapure water, and conditioned with 3 mL dilute HCl (<0.01 mol L^{-1}; pH 2–3) + 1% H$_2$O$_2$ twice prior to any use. Then the sample dissolved in 1 ml dilute (<0.01 mol L^{-1}; pH 2–3) hydrochloric acid was added with 33 μL hydrogen peroxide and immediately loaded onto the column. Under such conditions, vanadium partitions strongly onto the anion-exchange resin (Fukasawa and Yamane, 1977; Kiriyama and Kuroda, 1983; Nielsen et al., 2011). Residual matrix elements that were not entirely eliminated in the cation-exchange step were eluted in 15 mL dilute HCl (<0.01 mol L^{-1}; pH 2–3) + 1% H$_2$O$_2$. Vanadium was then collected with 17 mL 1 mol L^{-1} HCl and 3 mL 6 mol L^{-1} HCl.

To fully remove residual Cr, the anion-exchange procedure was further run with a clipped PE pipet filled with 100 μL of AG1-X8 (200–400 mesh) chloride-form anion resin. After cleaning with 2 mL 6 mol L^{-1} HCl, 2 mL of 1 mol L^{-1} HNO$_3$ and 2 mL of ultrapure water, and conditioned with 0.5 mL weak HCl (<0.01 mol L^{-1}; pH 2–3) + 1% H$_2$O$_2$ twice, the column was loaded with the sample dissolved in 1 mL dilute HCl (<0.01 mol L^{-1}; pH 2–3) + 1% H$_2$O$_2$ and washed with 2 mL dilute HCl (<0.01 mol L^{-1}; pH 2–3) + 1% H$_2$O$_2$. Vanadium was then collected with 1.7 mL 1 mol L^{-1} HCl and 0.3 mL 6 mol L^{-1} HCl. Then the purified V was dried down and dissolved in 2% (m/m) HNO$_3$ prior to isotope measurements by MC-ICP-MS. Total procedure blank (from sample dissolution to instrumental analysis) was <1.5 ng,

which is negligible compared with the amount of V used in the measurement (5–10 μg).

2.3. Mass spectrometry

Vanadium isotopic measurements were performed on a Thermo Scientific Neptune Plus MC-ICP-MS in the CAS Key Laboratory of Crust-Mantle and Environments at the University of Science and Technology of China (USTC), Hefei, China. An aliquot of the AA standard solution employed by Nielsen et al. (2011) and Prytulak et al. (2011) was used as a reference. Measurements were run in medium-resolution mode (resolution > 5500) with Jet sampling and Ni X-skimmer cones. The peaks of target isotope (like ^{50}V$^+$, ^{52}Cr$^+$, and ^{53}Cr$^+$) can be partially resolved from molecular interferences (such as ^{36}Ar^{14}N$^+$, ^{36}Ar^{16}O$^+$, ^{38}Ar^{14}N$^+$) with a flat-topped shoulder on the lower mass side of the mixed peaks (Fig. 3). The cup configuration and instrument parameters are summarized in Table 2. To get a high-intensity signal for the minor isotope (^{50}V), ^{51}V was measured with a 10^{10} Ω amplifier. Ti isotopes (^{48}Ti and ^{49}Ti) and Cr isotopes (^{52}Cr and ^{53}Cr) were also simultaneously collected for correcting the isobaric effects of ^{50}Ti and ^{50}Cr on ^{50}V (Table 2). The idle time was set at 3 s.

The sample and standard solutions were diluted in 2% (m/m) HNO$_3$. The typical sensitivity of ^{51}V was ~200 V/ppm under dry plasma using Aridus II desolvator (CETAC Technologies), which is much higher than previous work (~50 V/ppm, Nielsen et al., 2011). Thus the amount of V needed for a single analysis is significantly reduced (~0.8 ppm versus 5 ppm from Nielsen et al., 2011). The data were collected for 40 cycles
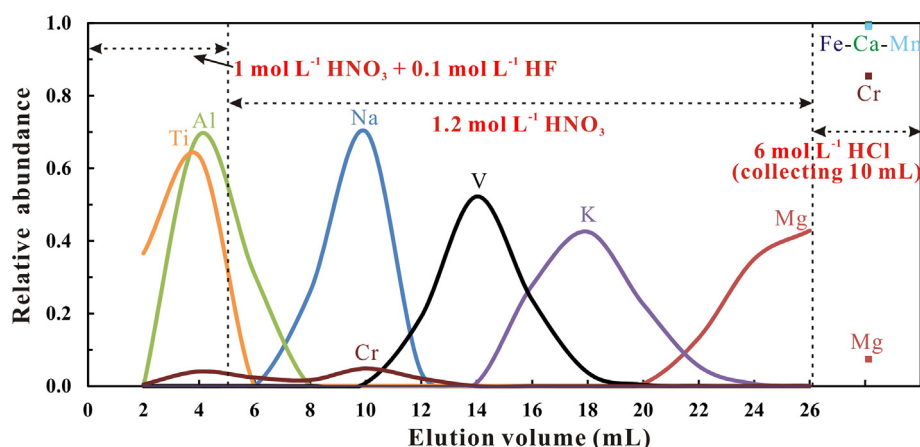

Fig. 1. Elution sequence of matrix elements and V from the AG50W-X12 (200–400 mesh) cation resin column. The igneous rock standard BIR-1 was used to obtain the elution curve.
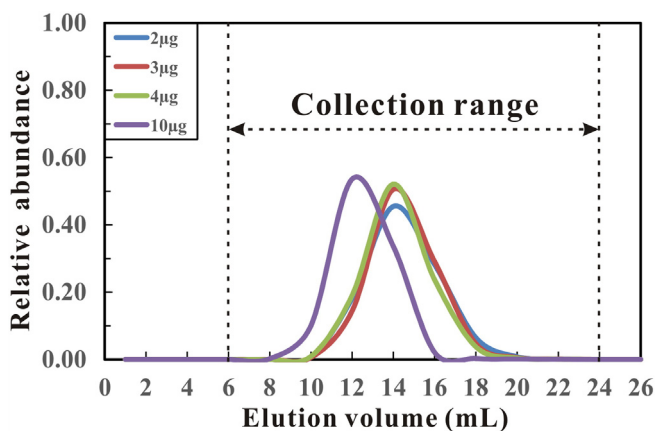
Fig. 2. Drifting of V elution curves with different masses of V loaded to the columns. Different amount of the BCR-2 powders were used to obtain the elution curves.

Table 2
Instrumental operating conditions for V isotopic measurements.

MC-ICP-MS	Thermo Fisher Scientific, Neptune Plus				
Cooling Ar	~16 L min^{-1}				
Auxiliary Ar	~0.8 L min^{-1}				
Nebulizer Ar	~0.85 L min^{-1}				
RF power	1160–1200 W				
Mass resolution	Medium resolution (resolution > 5500)				
Typical sensitivity	~200 V ppm^{-1} for ^{51}V				
Cones	Ni Jet cone, X-skimmer cone				
Desolvator	Aridus II				
Argon flow rate	~ 3.82 mL min^{-1}				
Installed nebulizer	Teflon self-aspirating micronebulizer system				
Solution uptake	~50 μL min^{-1}				
Detector mode	Faraday cup static mode				
	L4-F	L2-F	L1-F	C-F	H2-F	H3-F
Amplifier resistor	10^{11} Ω	10^{11} Ω	10^{11} Ω	10^{10} Ω	10^{11} Ω	10^{11} Ω
	^{48}Ti	^{49}Ti	^{50}V	^{51}V	^{52}Cr	^{53}Cr

with an integration time of 4.194 s per cycle. Every sample was bracketed by the AA standard solution before and after each single measurement, and the analyses were repeated ≥3 times for the same sample solution. Between each measurement, the sample introduction system was cleaned using 5% HNO$_3$ (m/m, 60 s) and then 2% HNO$_3$ (m/m, 60 s) to eliminate potential cross-contamination between each measurement. The ^{51}V background was lower than 30 mV after the washout procedure. On-peak zero correction was carried out for every analysis.

3. Accuracy and precision

3.1. Effects of sample/standard, acid molarity, and concentration mismatch

As shown in previous studies, mismatch in the acidity and concentration between samples and bracketing standards may cause artifacts in metal stable isotope analyses when using the sample-standard

bracketing method (e.g., An et al., 2014; He et al., 2015; Liu et al., 2014; Malinovsky et al., 2003). Thus, it is important to assess the potential influences of these two issues. To test the effect of acid molarity on V isotopic analysis, the AA solution was diluted to 800 ppb with 1% (m/m) to 3.2% (m/m) HNO$_3$, and then bracketed by the same standard solution diluted in 2% (m/m) HNO$_3$. As shown in Fig. 4 and Table 3, the differences in acid concentration between the standards and samples do not cause measurable isotopic deviation from the true value. In addition, because 2% (m/m) HNO$_3$ was always used to prepare samples and bracketing standards, acidity mismatch should not cause any artificial δ^{51}V value.

To determine the effect of V concentration in solution on V isotopic analysis, the AA standard solutions with concentrations ranging from ~600 to ~950 ppb were measured against bracketing standards at a constant V concentration (800 ppb) in a medium-resolution mode. Our results show that concentration mismatch does not influence V isotope analyses when the standard/sample concentration ratios range from
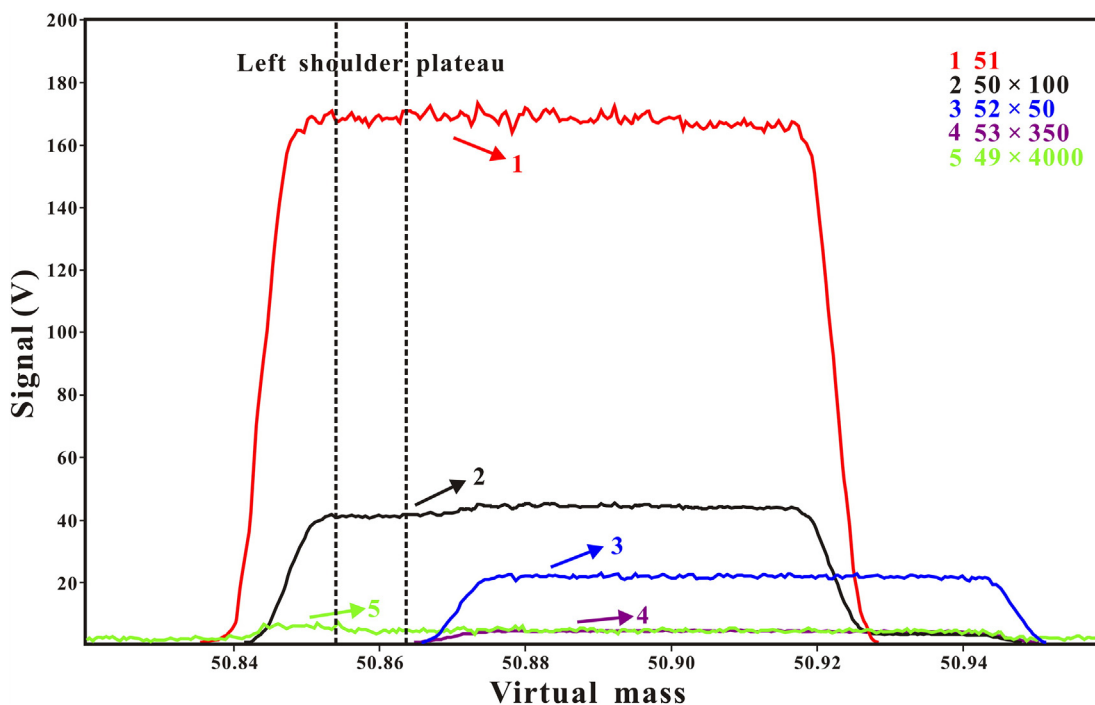
Fig. 3. Mass scan of ^{49}Ti, ^{50}V, ^{51}V, ^{52}Cr, and ^{53}Cr under medium-resolution mode using the dry plasma inlet system. In particular, the signals of ^{50}V, ^{52}Cr, and ^{53}Cr and their respective molecular interferences are shown here. Vanadium isotope ratios were measured on the left shoulder plateau to avoid the interferences. The BDH solution (800 ppb) was used for the demonstration.
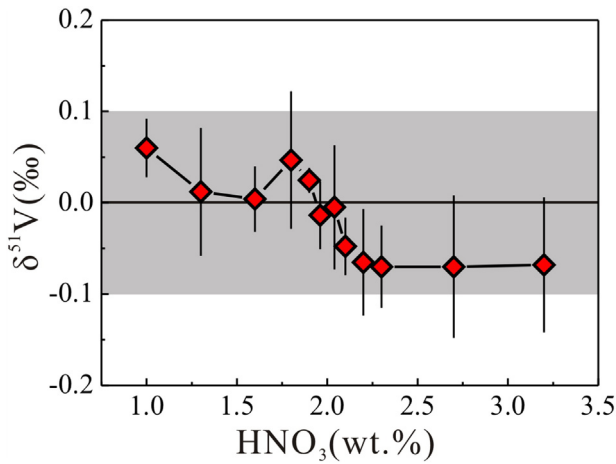
Fig. 4. The $\delta^{51}V$ variations of V standard solutions diluted by HNO_3 at different molarities. The error bars (2 SD) are based on at least three replicate measurements. The HNO_3 molarities in this test changed from 1% to 3.2% (m/m) (Table 3).

0.8 to 1.2 (Fig. 5 and Table 3). Nevertheless, the concentrations of sample solutions were adjusted to within 10% difference from the bracketing standard solution during the course of isotopic analysis.

3.2. Correction for Cr and Ti interferences

Because trace amounts of remaining Cr and Ti after purification dramatically affects ^{50}V measurements, ^{50}Cr and ^{50}Ti must be accurately corrected from the signal of mass 50. We assume that the instrumental mass fractionation of isotopes obeys the exponential law, i.e.:

$$R_T = R_M \times (m_1/m_2)^\beta, \tag{1}$$

where R_T and R_M refer to the true and measured isotope ratios of the same element, respectively, m_1 and m_2 are the masses of measured isotopes, and β is the mass fractionation factor.

To correct ^{50}Ti and ^{50}Cr, ^{49}Ti and ^{53}Cr were simultaneously measured. Here, the true value of $^{50}Ti/^{49}Ti$ and $^{50}Cr/^{53}Cr$ ratios are assumed to be 0.972537 (Leya et al., 2007) and 0.45737 (Nielsen et al., 2011; Shields et al., 1966), respectively. The β^{Ti} and β^{Cr} were estimated from the difference between the assumed true value of $^{50}Ti/^{49}Ti$ and $^{50}Cr/^{53}Cr$ ratios and the measured $^{50}Ti/^{49}Ti$ and $^{50}Cr/^{53}Cr$ ratios on a 100 ppb GSB Ti solution and a 100 ppb GSB Cr solution before each measurement sequence was started. Then, the interference of ^{50}Ti and ^{50}Cr during the sample analysis was calculated from the measured values of ^{49}Ti and ^{53}Cr through the equations shown below:

$$^{50}Ti_M = {}^{49}Ti_M \times \left({}^{50}Ti/^{49}Ti\right)_T / (50/49)^{\beta Ti} \tag{2}$$

and

$$^{50}Cr_M = {}^{53}Cr_M \times \left({}^{50}Cr/^{53}Cr\right)_T / (50/53)^{\beta Cr} \tag{3}$$

The β^{Ti} and β^{Cr} values vary in different analytical sessions (from -1.3 to -1.6) probably caused by the change of instrument state, but they are almost constant within one day's measurement.

Doping experiments of Cr and Ti were performed to confirm the safe range of Cr and Ti concentrations in solution below which the correction is valid for V isotopic analyses. The results are shown in Table 3 and Fig. 6, revealing that V isotope data of unknown samples were only considered to be valid when the sample has $^{53}Cr/^{51}V < 0.00004$ and $^{49}Ti/^{51}V < 0.00004$. Compared with the doping experiments from Nielsen et al. (2011), our results showed a large acceptable range for $^{53}Cr/^{51}V$, but a narrow range for $^{49}Ti/^{51}V$, which are probably caused by the different β value used in the analyses. In fact, most of the samples

Table 3
Influences of Cr and Ti doping, concentration and acid mismatch on V isotopic analyses.

Name		$\delta^{51}V$ (‰)	2 SD	n
Acid match	HNO_3 molarities (m/m)			
	1	0.06	0.03	3
	1.3	0.01	0.07	3
	1.6	0.00	0.04	3
	1.8	0.05	0.08	3
	1.9	0.02	0.01	3
	1.96	-0.01	0.04	3
	2.04	0.00	0.07	3
	2.1	-0.05	0.03	3
	2.2	-0.07	0.06	3
	2.3	-0.07	0.05	3
	2.7	-0.07	0.08	3
	3.2	-0.07	0.07	3
Concentration match test	$C_{sample}/C_{standard}$			
	0.76	-0.02	0.03	3
	0.84	-0.04	0.02	3
	0.89	-0.02	0.09	3
	0.95	-0.03	0.09	3
	0.97	-0.02	0.03	3
	1.02	0.02	0.03	3
	1.08	-0.04	0.03	3
	1.13	-0.01	0.03	3
	1.18	0.01	0.05	3
Cr doping test	$^{53}Cr/^{51}V$			
	0.000006	0.00	0.04	3
	0.000008	-0.01	0.10	2
	0.000016	-0.06	0.06	3
	0.000021	-0.06	0.06	4
	0.000028	-0.06	0.06	3
	0.000032	-0.08	0.05	4
	0.000051	-0.20	0.04	3
	0.000073	-0.23	0.06	3
	0.000108	-0.37	0.10	3
	0.000182	-0.56	0.13	4
	0.001201	-4.04	0.18	3
Ti doping test	$^{49}Ti/^{51}V$			
	0.000002	0.00	0.06	5
	0.000003	-0.01	0.08	3
	0.000006	-0.03	0.06	3
	0.000008	0.01	0.07	4
	0.000014	0.03	0.05	4
	0.000018	0.04	0.08	4
	0.000024	-0.06	0.02	3
	0.000028	0.05	0.11	4
	0.000041	-0.09	0.07	4
	0.000048	-0.13	0.07	3
	0.000499	0.91	0.21	3

n is the times of repeated measurements.
2 SD = 2 times the standard deviation of the population of n repeat measurements.

have $^{53}Cr/^{51}V$ and $^{49}Ti/^{51}V$ ratios below 0.00001 after our chemical purification procedure, so we can be sure that the Cr and Ti interferences did not cause artifacts in V isotope analyses using our method.

3.3. Precision and accuracy

In this study, we used three ways to show the precision and accuracy of V isotope analyses. First, two solution standards (BDH and USTC-V) were repeatedly measured relative to the AA standard solution to evaluate the long-term external reproducibility of pure V solution measurement of the instrument. The BDH solution is from an aliquot of the V solution employed by Nielsen et al. (2011) and Prytulak et al. (2011) as an in-house standard. The USTC-V, also used as an in-house standard, was prepared by mixing two bottles of ultrapure single element V solution (1000 μg mL^{-1}; in 0.5 mol L^{-1} HNO_3; 50 mL per bottle) named GSB, purchased from NCATN (Beijing, China). Second, different kinds of synthetic solutions were run to ensure that there was no isotope fractionation during chemical separation and instrumental measurement. Third, the accuracy of our method was verified by comparing $\delta^{51}V$ of
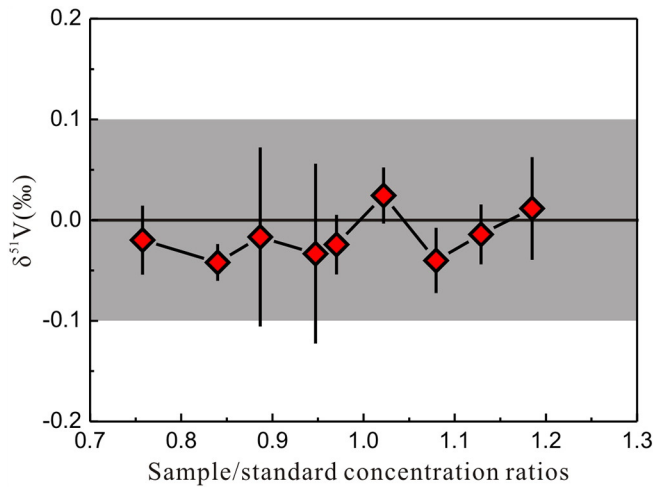
Fig. 5. The effect of sample/standard concentration mismatch on δ^{51}V analyses. Data are reported in Table 3.

standards (BIR-1, BHVO-2, BCR-2, AGV-2, and GSP-2) measured in our lab with the values reported in the literature (Prytulak et al., 2011).

Long-term analyses of the BDH solution over a period of more than 1 year gave an average δ^{51}V of -1.23 ± 0.08‰ (2 SD, $n = 197$) relative

to AA (Fig. 7), which is in agreement within uncertainty with that reported by Nielsen et al. (2011) (-1.19 ± 0.12‰). The long-term measurements of USTC-V gave an average δ^{51}V of $+0.07 \pm 0.08$‰ (2 SD, $n = 112$) relative to the AA solution (Fig. 7).

To ensure that there is no isotope shift during chemical separation and instrumental measurement, pure V standard solutions (BDH and USTC-V) and a set of synthetic solutions were treated with the whole-column chemistry. The purified solutions were then analyzed using MC-ICP-MS. The results are summarized in Table 4 and Fig. 8. The average δ^{51}V of pure BDH and USTC-V standard solutions after the column purification procedure are -0.02 ± 0.08‰ (2 SD, $n = 18$, relative to BDH) and -0.03 ± 0.06‰ (2 SD, $n = 12$, relative to USTC-V), respectively. The synthetic solution was made by mixing USTC-V with some other elements (V:Ti:Cr:Ca:Mg:Fe:Al:Na:Mn:Zn:Ni:Rb:Cu = 1:5.5:5.5:5.5:5.5:5.5:5.5:5.5:5.5:1.3:1.3:1.3:1.3). The average δ^{51}V of the synthetic solution relative to USTC-V is -0.01 ± 0.09‰ (2 SD, $n = 12$). In addition, we also mixed matrix solutions free of element V from separation steps of rock standards (including BIR-1, BCR-2, AGV-2, and NOD-P) with USTC-V solution to make synthetic standards. Measurement of solutions made by mixing USTC-V with a matrix of different reference materials all obtained values close to 0‰ relative to the pure USTC-V with a precision better than ± 0.1‰ (2 SD) (Table 4 and Fig. 8). Thus, these results verify that the chemical procedure and instrumental analyses did not produce measurable artifacts.

The precision and accuracy of our method were also assessed by repeating the measurements of the rock standards, including the same solution measured in different sessions and independent digestions of the same sample powders. The δ^{51}V values of the standards are listed in Table 5 and Fig. 9. The igneous rock standards BIR-1, BHVO-2, BCR-2, AGV-2, and GSP-2 have average δ^{51}V $= -0.92 \pm 0.09$‰ (2 SD, $n = 52$), δ^{51}V $= -0.83 \pm 0.09$‰ (2 SD, $n = 22$), δ^{51}V $= -0.78 \pm 0.08$‰

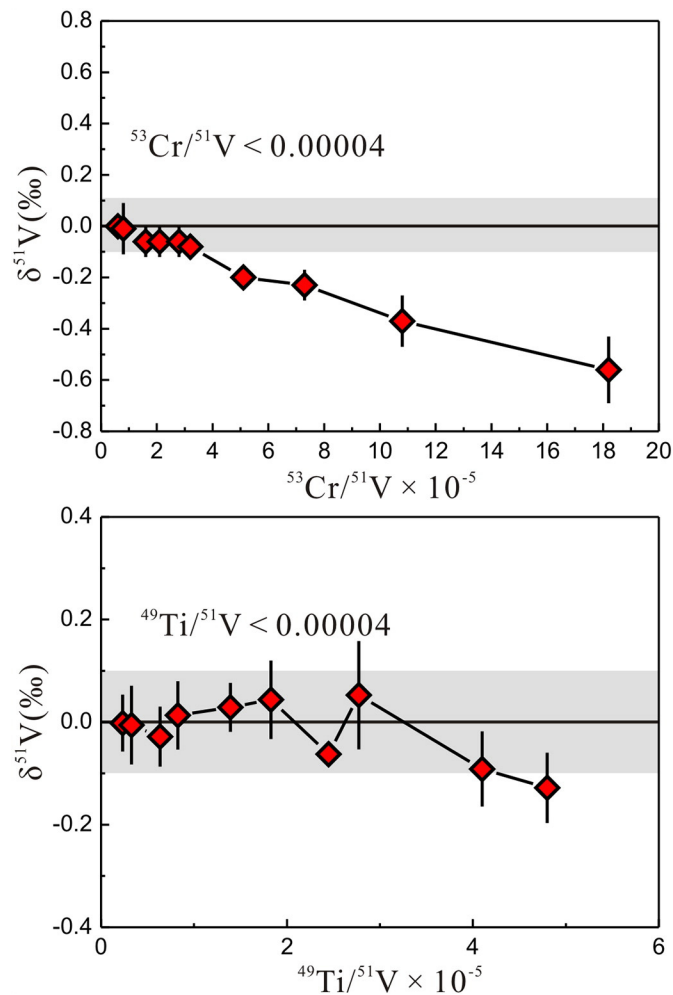**Fig. 6.** Doping experiments to test the V isotopic offsets generated by Ti and Cr correction. The δ^{51}V values are plotted versus ^{53}Cr/^{51}V (top panel) and ^{49}Ti/^{51}V (bottom panel) ratios in run solutions with different contents of Cr or Ti. V concentrations for samples and bracketing standards (USTC-V) are the same (800 ppb). Data are reported in Table 3.
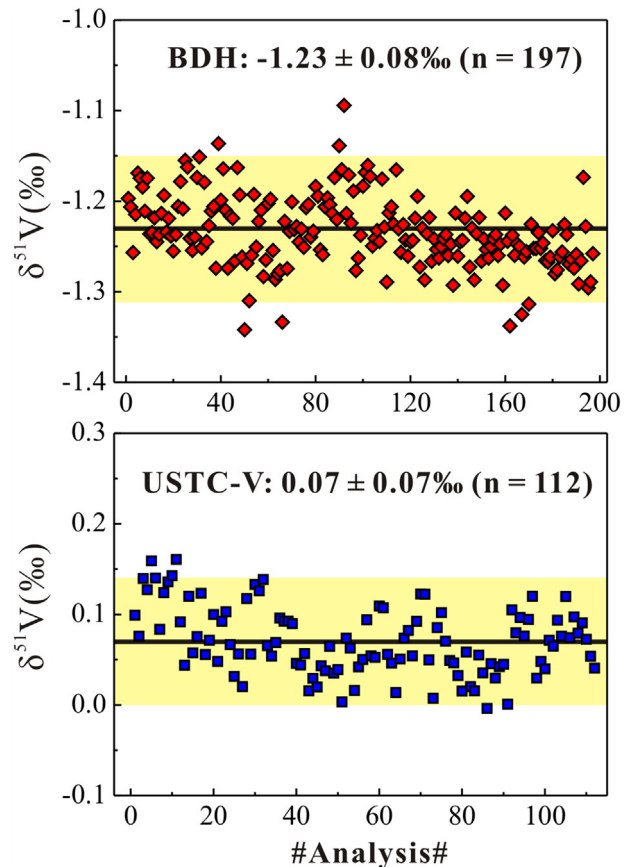

Fig. 7. The δ^{51}V values of BDH (top panel) and USTC-V (bottom panel). The long-term external precision is better than ± 0.1‰ (2 SD).

Table 4
Isotope shift during chemical separation and instrumental measurements.

Sample	Sample description	δ^{51}V (‰)	2 SD	n
BDH[a]	Pure solution	−0.02	0.07	7
		0.02	0.05	4
		−0.05	0.07	4
		−0.01	0.01	3
Average		−0.02	0.08	18[b]
USTC-V[c]	Pure solution	−0.03	0.05	6
		−0.01	0.03	3
		−0.05	0.07	3
Average		−0.03	0.06	12[b]
Synthetic solution[c]	USTC-V	−0.06	0.07	3
	(mixing with matrix elements)	0.03	0.10	3
		0.00	0.04	5
		−0.03	0.07	6
		0.01	0.09	9
Average		−0.01	0.09	26[b]
USTC-V[c] (matrix spiking)	NOD-P matrix spiking	0.02	0.04	3
	BCR-2 matrix spiking	0.06	0.09	3
	BIR-1 matrix spiking	0.01	0.08	3
	AGV-2 matrix spiking	−0.05	0.02	3

n is the times of repeated measurements of the same solution.
2 SD = 2 times the standard deviation of the population of n repeated measurements.
[a] δ^{51}V is reported relative to BDH V standard solution.
[b] The total number of repeated runs of the same sample including different column procedures.
[c] δ^{51}V is reported relative to USTC-V standard solution.

(2 SD, $n = 36$), δ^{51}V $= -0.70 \pm 0.10$‰ (2 SD, $n = 37$) and δ^{51}V $= -0.62 \pm 0.07$‰ (2 SD, $n = 26$), respectively. These δ^{51}V values are in agreement within uncertainty with those reported in Prytulak et al. (2011) (−0.94 ± 0.15‰ for BIR-1, −0.89 ± 0.08‰ for BHVO-2, −0.95 ± 0.16‰ for BCR-2, −0.50 ± 0.19‰ for AGV-2 and −0.63 ± 0.10‰ for GSP-2). In conclusion, the long-term external precision of our method is better than ±0.1‰ (2 SD) for δ^{51}V based on replicated analyses of pure V standards, synthetic solutions, and reference materials.

4. δ^{51}V of igneous rock and manganese nodule standards

Twelve international reference materials were analyzed in this study, including 10 igneous rock standards (basalt: BCR-2, BHVO-2, BIR-1 and JB-2; diabase: W-2; andesite: AGV-1, AGV-2 and JA-2; quartz latite: QLO-1; and granodiorite: GSP-2) and two manganese nodule standards (NOD-P and NOD-A). As Table 5 and Fig. 9 show, δ^{51}V in the igneous rock standards vary by 0.33‰, larger than the error of our method (2 SD, 0.1‰). In addition, δ^{51}V of igneous rock standards are positively correlated with SiO$_2$ and negatively with V contents
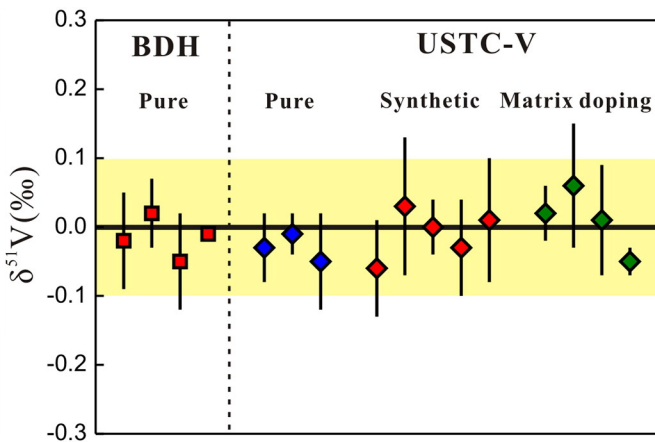

Fig. 8. The δ^{51}V values of pure solution, element doping, and matrix spiking tests relative to the pure solutions (BDH or USTC-V). Such tests all obtained values close to the ideal value (0‰) with the precision better than ±0.1‰ (2 SD). Data are reported in Table 4.

Table 5
V isotopic composition of standards.

Sample	Sample description	δ^{51}V (‰)	2 SD	n
BIR-1	Standard (basalt)	−0.94	0.02	4
		−0.95	0.08	4
		−0.89	0.05	7
		−0.92	0.13	7
		−0.97	0.05	8
		−0.96	0.04	4
		−0.91	0.08	3
		−0.89	0.08	3
		−0.97	0.04	2
		−0.89	0.06	10
Average		−0.92	0.09	52[a]
Literature		−0.94	0.15	52
BHVO-2	Standard (basalt)	−0.87	0.09	4
		−0.79	0.03	4
		−0.82	0.08	4
		−0.84	0.03	4
		−0.81	0.07	3
		−0.87	0.12	3
Average		−0.83	0.09	22[a]
Literature		−0.89	0.08	9
BCR-2	Standard (basalt)	−0.76	0.10	7
		−0.78	0.07	7
		−0.79	0.03	3
		−0.80	0.07	7
		−0.79	0.11	6
		−0.76	0.08	6
Average		−0.78	0.08	36[a]
Literature		−0.95	0.16	27
JB-2	Standard (basalt)	−0.90	0.08	3
		−0.86	0.05	6
		−0.86	0.07	3
		−0.86	0.03	8
Average		−0.87	0.06	20[a]
W-2	Standard (diabase)	−0.93	0.10	4
		−0.95	0.08	5
		−0.92	0.05	3
		−0.95	0.12	3
Average		−0.94	0.08	15[a]
AGV-1	Standard (andesite)	−0.67	0.02	3
		−0.75	0.02	3
Average		−0.71	0.10	6[a]
AGV-2	Standard (andesite)	−0.68	0.08	4
		−0.67	0.07	7
		−0.75	0.11	7
		−0.73	0.06	7
		−0.70	0.06	6
		−0.64	0.05	3
		−0.69	0.07	3
Average		−0.70	0.10	37[a]
Literature		−0.50	0.19	4
JA-2	Standard (andesite)	−0.78	0.05	6
		−0.83	0.08	4
		−0.81	0.03	3
Average		−0.80	0.07	13[a]
GSP-2	Standard (granodiorite)	−0.62	0.04	8
		−0.56	0.06	4
		−0.62	0.07	6
		−0.63	0.03	5
		−0.63	0.08	3
Average		−0.62	0.07	26[a]
Literature		−0.63	0.10	6
QLO-1	Standard (quartz latite)	−0.61	0.03	3
Average		−0.61	0.03	3[a]
NOD-P	Standard (manganese nodule)	−1.67	0.03	4
		−1.63	0.05	6
Average		−1.65	0.06	10[a]
NOD-A	Standard (manganese nodule)	−0.93	0.05	6
		−1.04	0.05	7
		−0.99	0.05	6
Average		−0.99	0.10	19[a]

n is the times of repeated measurements of the same solution.
2 SD = 2 times the standard deviation of the population of n repeated measurements.
The literature results are from Prytulak et al. (2011).
[a] The total number of repeated runs of the same sample including different digestions.
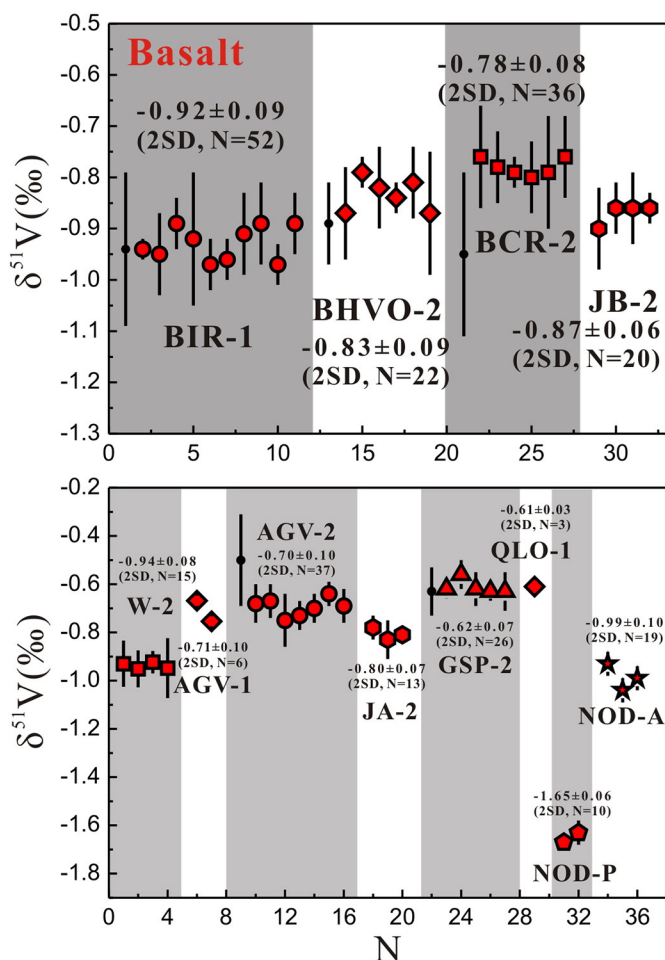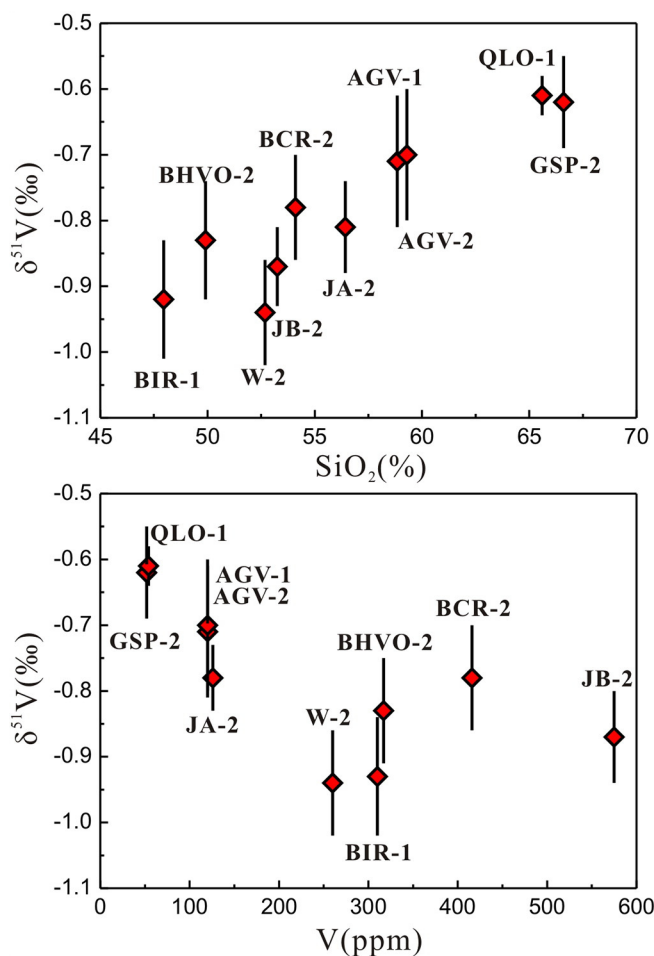
Fig. 9. The $\delta^{51}V$ values of silicate rock and manganese nodule standards. Solid small black circles represent results from Prytulak et al. (2011). Error bars reflect 2 standard deviations (2σ). Data are reported in Table 3.

Fig. 10. The $\delta^{51}V$ values of silicate rock standards versus SiO_2 and V contents. The $\delta^{51}V$ variations of these standards are positively correlated with SiO_2 and negatively with V contents, indicating that V isotope fractionation occurs during magmatic process.

(Fig. 10), confirming V isotope fractionation during magmatism as earlier observed by Prytulak et al. (2012). Such variations might be caused by isotope fractionation between V^{3+} and V^{4+} which show different partitioning behaviors between crystal and melt (e.g., Mallmann and O'Neill, 2009).

The two manganese nodule standards (NOD-P and NOD-A) show large V isotopic variations. As Table 5 shows, NOD-P has lighter $\delta^{51}V$ ($-1.65 \pm 0.06\text{‰}$, 2 SD, $n = 10$) than NOD-A ($-0.99 \pm 0.10\text{‰}$, 2 SD, $n = 19$). Such results show that V isotopes can be significantly fractionated in low-temperature processes.

5. Conclusions

We have developed a method for high-precision V isotopic ratio analyses by Neptune Plus MC-ICP-MS using the sample-standard bracketing method. The increase in instrument sensitivity significantly reduces the amount of V required for isotope analysis (~0.8 ppm versus 5 ppm from Nielsen et al., 2011). Vanadium was purified through an ion-exchange procedure using cation- and anion-exchange columns. This method improves time efficiency and eliminates the need for expensive TRU Spec resin. Vanadium isotopic compositions were measured using the Alfa Aesar (AA) V standard solution as the bracketing standard. The medium-resolution mode was used to avoid interference of molecular interferences (such as $^{36}Ar^{14}N^+$, $^{36}Ar^{16}O^+$, $^{38}Ar^{14}N^+$) with target isotope (like $^{50}V^+$, $^{52}Cr^+$, and $^{53}Cr^+$). Isobaric interferences of ^{50}Cr and ^{50}Ti were carefully corrected during the measurement.

Systematic testing showed no significant analytical artifact when the standard/sample concentration ratio ranged from 0.8 to 1.2 and the difference of acid concentration is less than 50%. Based on repeated measurements of pure V solutions and synthetic standards, the long-term external reproducibility is better than $\pm 0.1\text{‰}$ (2 SD) for $\delta^{51}V$.

Vanadium isotopic compositions of 12 international reference materials, including igneous rock standards and manganese nodules standards, were analyzed in this study. The overall variation of $\delta^{51}V$ in these standards is up to 1‰, confirming significant V isotope fractionation in nature (Nielsen et al., 2014; Prytulak et al., 2013; Ventura et al., 2015). The $\delta^{51}V$ of the igneous rock standards are positively correlated with SiO_2 and negatively with V contents, supporting the notion that V isotope fractionation might occur during high-temperature magmatic processes (Prytulak et al., 2012). Finally, the large V isotopic difference between the two manganese nodule standards shows that V isotopes can be significantly fractionated in low-temperature processes.

References

Algeo, T.J., Maynard, J.B., 2004. Trace-element behavior and redox facies in core shales of Upper Pennsylvanian Kansas-type cyclothems. Chem. Geol. 206, 289–318.

An, Y., Wu, F., Xiang, Y., Nan, X., Yu, X., Yang, J., Yu, H., Xie, L., Huang, F., 2014. High-precision Mg isotope analyses of low-Mg rocks by MC-ICP-MS. Chem. Geol. 390, 9–21.

Anbar, A.D., Jarzecki, A.A., Spiro, T.G., 2005. Theoretical investigation of iron isotope fractionation between $Fe(H_2O)_6^{3+}$ and $Fe(H_2O)_6^{2+}$: implications for iron stable isotope geochemistry. Geochim. Cosmochim. Acta 69, 825–837.

Baes, C.F., Mesmer, R.E., 1976. Hydrolysis of cations. Wiley.

Balsiger, H., Geiss, J., Lipschutz, M.E., 1969. Vanadium isotopic composition in meteoritic and terrestrial matter. Earth Planet. Sci. Lett. 6, 117–122.

Balsiger, H., Mendia, M.D., Pelly, I.Z., Lipschutz, M.E., 1976. Vanadium isotopic composition and contents in gas-rich meteorites. Earth Planet. Sci. Lett. 28, 379–384.

Breit, G.N., Wanty, R.B., 1991. Vanadium accumulation in carbonaceous rocks — a review of geochemical controls during deposition and diagenesis. Chem. Geol. 91, 83–97.

Canil, D., 2002. Vanadium in peridotites, mantle redox and tectonic environments: Archean to present. Earth Planet. Sci. Lett. 195, 75–90.

Ellis, A.S., Johnson, T.M., Bullen, T.D., 2002. Chromium isotopes and the fate of hexavalent chromium in the environment. Science 295, 2060–2062.

Fukasawa, T., Yamane, T., 1977. Determination of trace vanadium in natural waters by a combined ion exchange—catalytic photometric method. Anal. Chim. Acta 88, 147–153.

He, Y., Ke, S., Teng, F.-Z., Wang, T., Wu, H., Lu, Y., Li, S., 2015. High-precision iron isotope analysis of geological reference materials by high-resolution MC-ICP-MS. Geostand. Geoanal. Res. (n/a-n/a).

Huang, J.-H., Huang, F., Evans, L., Glasauer, S., 2015. Vanadium: global (bio)geochemistry. Chem. Geol. 417, 68–89.

Kiriyama, T., Kuroda, R., 1983. Anion-exchange separation and spectrophotometric determination of vanadium in silicate rocks. Talanta 30, 261–264.

Lee, C.-T.A., Aeolus, L., Leeman, C.T., Canil, W.P., LI, D., X.A, Z., 2005. Similar V/Sc systematics in MORB and arc basalts: implications for the oxygen fugacities of their mantle source regions. J. Petrol. 46, 2313–2336.

Leya, I., Schönbächler, M., Wiechert, U., Krähenbühl, U., Halliday, A.N., 2007. High precision titanium isotope measurements on geological samples by high resolution MC-ICPMS. Int. J. Mass Spectrom. 262, 247–255.

Liu, S.-A., Li, D., Li, S., Teng, F.-Z., Ke, S., He, Y., Lu, Y., 2014. High-precision copper and iron isotope analysis of igneous rock standards by MC-ICP-MS. J. Anal. At. Spectrom.

Malinovsky, D., Stenberg, A., Rodushkin, I., Andren, H., Ingri, J., Ohlander, B., Baxter, D.C., 2003. Performance of high resolution MC-ICP-MS for Fe isotope ratio measurements in sedimentary geological materials. J. Anal. At. Spectrom. 18, 687–695.

Mallmann, G., O'Neill, H.S.C., 2009. The crystal/melt partitioning of V during mantle melting as a function of oxygen fugacity compared with some other elements (Al, P, Ca, Sc, Ti, Cr, Fe, Ga, Y, Zr and Nb). J. Petrol. 50, 1765–1794.

Morford, J.L., Emerson, S., 1999. The geochemistry of redox sensitive trace metals in sediments. Geochim. Cosmochim. Acta 63, 1735–1750.

Nielsen, S.G., Prytulak, J., Halliday, A.N., 2011. Determination of Precise and Accurate 51 V/50 V Isotope Ratios by MC-ICP-MS, part 1: chemical separation of vanadium and mass spectrometric protocols. Geostand. Geoanal. Res. 35, 293–306.

Nielsen, S.G., Prytulak, J., Wood, B.J., Halliday, A.N., 2014. Vanadium isotopic difference between the silicate Earth and meteorites. Earth Planet. Sci. Lett. 389, 167–175.

Papike, J.J., Karner, J.M., Shearer, C.K., 2005. Comparative planetary mineralogy: valence state partitioning of Cr, Fe, Ti, and V among crystallographic sites in olivine, pyroxene, and spinel from planetary basalts. Am. Mineral. 90, 277–290.

Pelly, I.Z., Lipschutz, M.E., Balsiger, H., 1970. Vanadium isotopic composition and contents in chondrites. Geochim. Cosmochim. Acta 34, 1033–1036.

Prytulak, J., Nielsen, S.G., Halliday, A.N., 2011. Determination of precise and accurate 51 V/50 V isotope ratios by multi-collector ICP-MS, part 2: isotopic composition of six reference materials plus the allende chondrite and verification tests. Geostand. Geoanal. Res. 35, 307–318.

Prytulak, J., Nielsen, S.G., Ionov, D.A., Halliday, A.N., Harvey, J., Kelley, K.A., Niu, Y.L., Peate, D.W., Shimizu, K., Sims, K.W.W., 2013. The stable vanadium isotope composition of the mantle and mafic lavas. Earth Planet. Sci. Lett. 365, 177–189.

Prytulak, J., Savage, P., Halliday, A., 2012. Stable vanadium isotope fractionation during differentiation. Mineral. Mag. 76, A2254.

Schauble, E., Rossman, G.R., Taylor Jr., H.P., 2004. Theoretical estimates of equilibrium chromium-isotope fractionations. Chem. Geol. 205, 99–114.

Shields, W.R., Murphy, T.J., Catanzaro, E.J., Garner, E.L., 1966. Absolute isotopic abundance ratios and the atomic weight of a reference sample of chromium. J. Res. Natl. Bur. Stand. A 70, 193–197.

Shore, A., Fritsch, A., Heim, M., Schuh, A., Thoennessen, M., 2010. Discovery of the vanadium isotopes. At. Data Nucl. Data Tables 96, 351–357.

Siebert, J., Badro, J., Antonangeli, D., Ryerson, F.J., 2013. Terrestrial accretion under oxidizing conditions. Science 339, 1194–1197.

Takeno, N., 2005. Atlas of Eh-pH diagrams. Geological Survey of Open File Report. 102.

Ventura, G.T., Gall, L., Siebert, C., Prytulak, J., Szatmari, P., Hürlimann, M., Halliday, A.N., 2015. The stable isotope composition of vanadium, nickel, and molybdenum in crude oils. Appl. Geochem. 59, 104–117.

Wood, B.J., Wade, J., Kilburn, M.R., 2008. Core formation and the oxidation state of the earth: additional constraints from Nb, V and Cr partitioning. Geochim. Cosmochim. Acta 72, 1415–1426.

Wu, F., Qin, T., Li, X., Liu, Y., Huang, J.-H., Wu, Z., Huang, F., 2015. First-principles investigation of vanadium isotope fractionation in solution and during adsorption. Earth Planet. Sci. Lett. 426, 216–224.

Zhang, Y.-H., Ban, Y., Nomura, M., Fujii, Y., 2003a. Isotope effects in the V(IV)-malate complex formation system. Polyhedron 22, 1377–1383.

Zhang, Y.-H., Nomura, M., Aida, M., Fujii, Y., 2003b. Separation of vanadium isotopes by ion-exchange chromatography. J. Chromatogr. A 989, 175–182.

Zhou, X., Wei, C., Li, M., Qiu, S., Li, X., 2011. Thermodynamics of vanadium–sulfur–water systems at 298 K. Hydrometallurgy 106, 104–112.